



HAL
open science

Particle size effects on critical strength of granular soils through numerical and laboratory testing

Paula Quiroz Rojo, Carlos Ovalle, Gilbert Girumugisha, David Cantor, Emilien Azéma, Mathieu Renouf

► To cite this version:

Paula Quiroz Rojo, Carlos Ovalle, Gilbert Girumugisha, David Cantor, Emilien Azéma, et al.. Particle size effects on critical strength of granular soils through numerical and laboratory testing. Pan-American Conference on Soil Mechanics and Geotechnical Engineering (XVII PCSMGE), Nov 2024, La Serena, Chile. hal-04804353

HAL Id: hal-04804353

<https://hal.science/hal-04804353v1>

Submitted on 26 Nov 2024

HAL is a multi-disciplinary open access archive for the deposit and dissemination of scientific research documents, whether they are published or not. The documents may come from teaching and research institutions in France or abroad, or from public or private research centers.

L'archive ouverte pluridisciplinaire **HAL**, est destinée au dépôt et à la diffusion de documents scientifiques de niveau recherche, publiés ou non, émanant des établissements d'enseignement et de recherche français ou étrangers, des laboratoires publics ou privés.

Particle size effects on critical strength of granular soils through numerical and laboratory testing

Efectos de tamaño de partícula en la resistencia al corte crítica de suelos granulares mediante ensayos numéricos y de laboratorio.

Paula Quiroz Rojo^{1,2,3}, Carlos Ovalle^{2,3}, Gilbert Girumugisha^{2,3}, David Cantor^{2,3}, Emilien Azéma^{1,2,4}, Mathieu Renouf¹

¹ *Laboratoire de Mécanique et Génie Civil, Université de Montpellier, France. paula.quiroz-rojo@umontpellier.fr*

² *Department of Civil, Geological, and Mining Engineering, Polytechnique Montréal, Canada*

³ *Research Institute of Mining and Environment (RIME), UQAT-Polytechnique, Canada*

⁴ *Institut Universitaire de France (IUF), Paris, France.*

ABSTRACT: The critical shear strength characterization of waste rock (WR) is crucial for assessing the stability of waste rock piles. However, laboratory testing is challenging due to the broad grain size distribution (GSD) that ranges from silts to oversized rock clasts. The maximum grain size in a sample is restricted by the size of the equipment and the recommendations by international standards. This implies that WR materials require their GSD to be altered using grading scaling techniques to fit into standard testing cells. The common geotechnical practice for scaling is based on the aspect ratio $\alpha = D/d_{max}$, where D is the diameter of the sample and d_{max} the maximum grain diameter. However, different standards disagree on the minimum α to ensure a representative sample, ranging from $\alpha = 5$ to 20. The main objective of this paper is to study the effects of α on the critical shear strength of granular materials through numerical triaxial tests in the frame of the discrete-element method (DEM) and laboratory triaxial tests on WR material. The samples used have α values varying from 5 to 20 and GSD of uniformity coefficients ranging from $C_u = 1$ to 2.2. The results show that the numerical and physical samples exhibit stable critical strength for $\alpha \geq 12$, regardless their initial grading. These results demonstrate the advantages of numerically testing materials that are challenging to fit into standard devices and suggest that international standards should be revisited to include the significant effects of α .

KEYWORDS: shear strength, DEM, mine waste rock, size effect.

1 INTRODUCTION.

Waste rocks (WR) are the valueless portion extracted to mine the ore, and their grain size distribution (GSD) includes a variety of particles, from silts up to clasts with more than 1 m in diameter (Bard et al., 2012; Ovalle et al., 2020). WR form waste rock piles which are recognized as one of the highest man-made geo-structures (Valenzuela et al., 2008). However, WR piles present high environmental risks and uncertain mechanical stability. To ensure the latter, extensive laboratory testing should be carried out to provide mechanical WR characterization (Linero et al., 2007, 2020; Ovalle et al., 2023). Due to the coarse rock clasts, the GSD must be altered according to the testing device available. Two small-scaling techniques are the most used: parallel grading (Marachi et al, 1972) and scalping (Zeller & Wulliman, 1957). In parallel grading, the shape of the GSD curve is preserved by scaling down both maximum (d_{max}) and minimum (d_{min}) particle sizes. In scalping, the material coarser than a size d_{max} is removed and a new GSD curve is generated by truncating the original one. Small-scaling methods are expected to provide representative results on the basis that critical shear strength does not depend on the GSD, as widely shown via experimental and numerical studies (Li et al., 2013; Yang and Luo, 2017; Azéma et al., 2017; Amirpour et al., 2019; Cantor et al., 2020). However, the scaling methods require that particle roughness and characteristic

particle shape remain relatively constant in small-scaled samples (Ovalle and Dano, 2020; Carrasco et al., 2022, 2023).

Typically, triaxial or direct shear tests are used to measure the shear strength, applying d_{max} restrictions according to international testing standards (Cantor and Ovalle, 2023; Girumugisha et al., 2024). For triaxial tests, considering the sample aspect ratio $\alpha = D/d_{max}$, where D is the sample diameter, the values recommended are 5, 6 and 20, after British (BS 1377), American (ASTM D7181) and Japanese (JGS 0520) testing standards, respectively. Disagreement between the standards shows that the effects of α and GSD on the mechanical behavior are still poorly understood.

The main objective of this paper is to study the effects of α on the critical shear strength of granular materials. The recommended limits of α imposed by international standards are tested through triaxial numerical tests, in the frame of the discrete-element method (DEM), and triaxial laboratory tests on WR materials.

2 METHODOLOGIES

2.1 Numerical DEM triaxial testing

Drained triaxial 3D simulations on spheres are carried out using the simulation platform LMGC90, developed at the University of Montpellier, France. LMGC90 uses the non-smooth discrete-element approach known as contact dynamics (Dubois & Jean,

2006), which is capable of simulating interactions between rigid grains of varied shapes and sizes. The density of the solid material and the inter-particle friction coefficient are set to $\rho = 2000 \text{ kg/m}^3$ and $\mu_s = 0.4$, respectively.

A rigid wall box of width $W = 0.1 \text{ m}$ and ratio $H/W = 2$ is modeled, where H is the box's height. It is worth noting that this configuration is similar to a true triaxial test (Hambly, 1969), therefore different from the stress field generated by flexible membranes in standard triaxial testing. This configuration was simply chosen due to lower computational cost. A series of α are chosen to cover the values recommended by testing standards: $\alpha = [5, 6, 8, 10, 12, 15, 17.5, 20]$. The GSD is characterized by the parameter $R_d = d_{max}/d_{min}$, and the following values are modeled: $R_d = [1.0, 1.1, 1.8, 4]$, which correspond to $C_u = d_{60}/d_{10} = [1.0, 1.1, 1.4, 2.2]$, respectively. Thus, d_{max} is given by the α value chosen and d_{min} by a given R_d . The GSDs are shown in Fig. 1, where (a) presents different C_u values for a given α , and (b) shows eight parallel curves for a given $C_u = 1.4$, corresponding to the eight values of α proposed. 32 different samples are simulated in total. As an example, Fig. 2 presents screenshots of two samples, for combinations of small and large values for α and C_u .

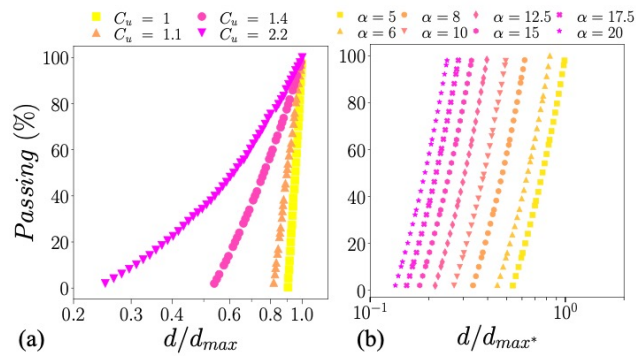


Figure 1. GSD of the numerical samples: (a) four C_u simulated for each α ; (b) parallel GSDs with $C_u = 1.4$ covering a wide range of α .

The numerical triaxial tests are performed in two stages. First, the samples are compressed with a constant stress $\sigma_0 = 10 \text{ kPa}$, applied through rigid walls. To avoid stress gradients and boundary effects, the friction coefficient between the walls and the particles is null. This stage is carried out until the variation of the void ratio is less than 0.1%. The second stage is the triaxial shearing, which is undertaken by applying a constant velocity v_z on the top and bottom walls of the box, keeping constant the confining pressure through lateral rigid walls. The value of the velocity is calculated based on the inertial number $I = d_{max}(v_z/H_0)/\sqrt{\rho/\sigma_0} \ll 1$ (GDR MiDi, 2004), where H_0 is the height of the sample after isotropic compression. The inertial number is fixed for all the samples at $I = 10^{-4}$, to ensure a quasi-static shearing regime. Finally, the tests were finished when the deformation of the sample reached 60% of H_0 .

2.2 Physical triaxial testing

A material called WR1 was collected from a hard rock mine. The material has a specific gravity of $G_s = 2.75$ and a uniaxial

compression strength of $UCS = 128 \text{ MPa}$. Mineralogy of WR1 is mainly composed of silicates (quartz and albite). Fig. 3a presents the GSD of the field material ($d_{max} = 75 \text{ mm}$), as well as scalped samples of WR1 down to d_{max} from 19 to 5 mm. The material classifies as a well-graded gravel with silt and sand (GW-GM). Additionally, a second set of samples (WR2, shown in Fig. 3b) is prepared from WR1, after removing all the fines ($< 0.08 \text{ mm}$) and particles coarser than 19 mm. The scalping technique is also applied to prepare small-scaled samples of WR2, as shown in Fig. 3b. Each sample is tested on triaxial specimens of diameter $D = 150 \text{ mm}$, which allowed to accommodate different aspect ratios α , from 6 to 30.

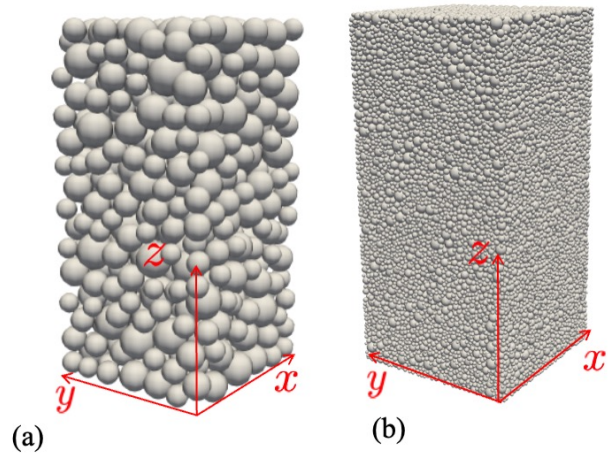


Figure 2. Examples of two samples tested: (a) $(\alpha, C_u) = [5, 1.0]$; (b) $(\alpha, C_u) = [15, 2.2]$.

Characteristic particle shape of the WR material is characterized through width to length sphericity $S_{WL} = \text{particle width/particle length}$, and roundness $R = \sum(r_i/N)/r_{in}$, where r_i is the radius of circles fitting the particle's concave corners, N the number of the fitted circles, and r_{in} the radius of the largest inscribed circle (Zheng and Hryciw, 2015). The results show that characteristic particle shapes are relatively constant over the whole range of particle sizes, with $R = 0.3$ to 0.4 and $S_{WL} = 0.7$, which classify as subangular particles with low sphericity.

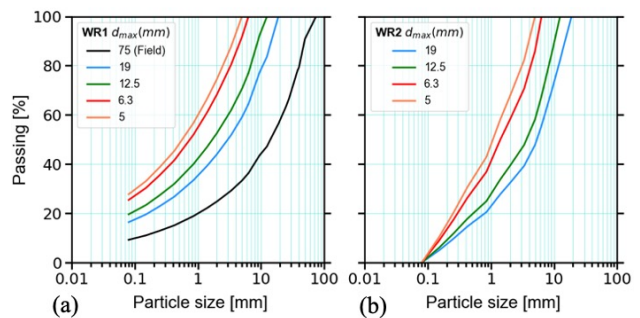


Figure 3. GSD of WR materials scalped for testing: (a) WR1 and (b) WR2.

Triaxial tests under consolidated drained conditions were performed on cylindrical dry specimens of $D = 150$ mm and $H = 300$ mm. A total of 18 tests are carried out on WR1 samples, and 15 on WR2. Loose samples are prepared without compaction by simply pouring the material into 10 distinct layers of homogeneous materials. Approximately 1.0 kg per layer is used. Dry densities obtained are different since the GSD varied between scalped samples. Dry densities of WR1 and WR2 varied between $17.83 - 18.95$ kN/m³, and $18.57 - 18.95$ kN/m³, respectively. An isotropic consolidation stage was performed by maintaining a desired confinement stress, varying between 45 to 210 kPa.

3 RESULTS

3.1 Numerical results

The discrete-element approach for simulations allows us to determine the inter-granular forces and stresses, which are useful to estimate the deviatoric stress $q = \sigma_1 - \sigma_3$ and the mean pressure $p = (\sigma_1 + 2\sigma_3)/3$ during triaxial shearing. This is based on the construction of a granular stress tensor computed through contact forces and particle positions (Ouaïfadel and Rothenburg, 2001; Radjai and Dubois, 2011).

In Fig. 4, the evolution of q/p and volumetric deformation (ε_v) are shown for all cases with $C_u = 2.2$ as a function of vertical deformation ε_1 . A clear peak of q/p is reached around 10 % of deformation, and the specimen shows dilatant behavior followed by a critical state. Fig. 5 illustrates that, regardless of the GSD, the values of critical state friction angle ϕ_{cr} stabilize only if $\alpha \geq 12$. Moreover, better graded samples ($C_u = 1.4 - 2.2$) result in steady values of ϕ_{cr} at $\alpha \geq 8$. Laboratory triaxial tests also indicate that the critical shear strength is stable only if $\alpha \geq 12$.

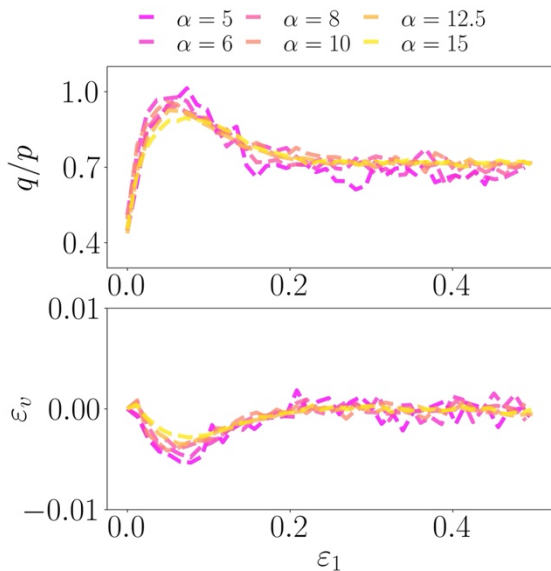


Figure 4. Normalized shear strength q/p and volumetric deformation ε_v as a function of the vertical deformation ε_1 for samples with $C_u = 2.2$

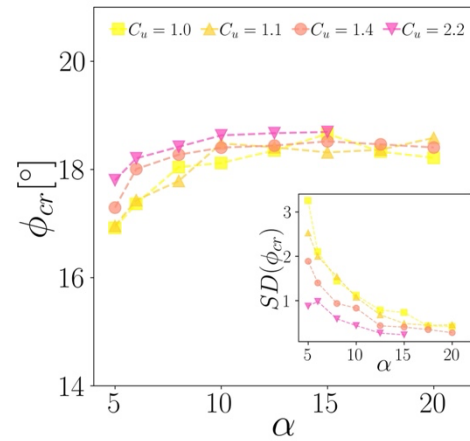


Figure 5. Critical friction angle ϕ_{cr} as a function of α

3.2 Physical experimental results

Fig. 6 shows the stress ratios q/p against ε_1 for all the triaxial tests. For each material, tests are grouped by confining pressure σ_3 . As expected on loose samples, all tests exhibit hardening and reached their maximum strength around $\varepsilon_1=10\%$, which remains almost constant up to $\varepsilon_1=15\%$. Loose samples of WR1 present slight dilation at low σ_3 of 45 and 80 kPa, which vanishes to fully contractive behavior for $\sigma_3 \geq 150$ kPa.

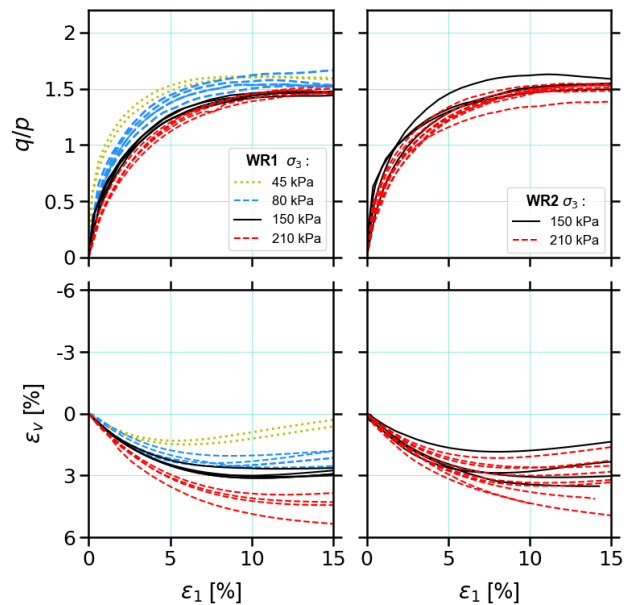


Figure 6. Normalized shear strength q/p results and volumetric deformation of the tested WRs, as a function of vertical deformation ε_1

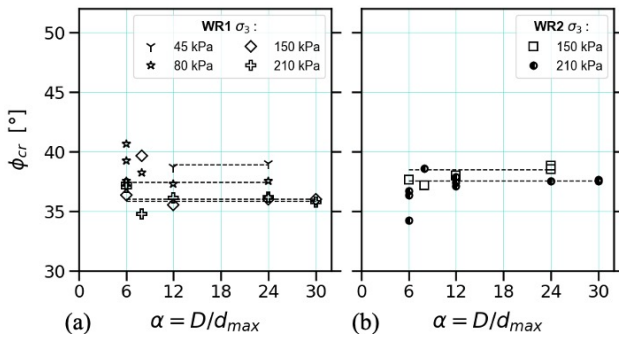


Figure 7. Critical friction angle comparison at different confinement pressure. (a) and (b) correspond with the two tested materials.

All q/p values reached at large vertical strain in Fig. 5 tend to similar values, which is consistent with several reported experimental results indicating that critical strength does not depend on PSD. However, the effect of α cannot be clearly identified in the figure. Therefore, Fig. 7 presents the critical friction angle (ϕ_{cr}) for all tests as a function of α , where dashed lines represent the mean ϕ_{cr} for each confining pressure σ_3 . For comparison, ϕ_{cr} is assumed to be the mobilized shear strength at $\varepsilon_1=15\%$ and calculated according to the Mohr-Coulomb failure criterion for non-cohesive materials. Samples tested at $\sigma_3=150$ kPa exhibit mean ϕ_{cr} of 36° and 38° for WR1 and WR2, respectively. It can be observed that, for a given σ_3 , ϕ_{cr} is stable for α between 12 and 30 but presents dispersion (of about 3°) at $\alpha < 12$. To highlight the scatter of ϕ_{cr} on all samples, Fig. 8 illustrates the ratio $\phi_{cr}/\phi_{cr(\alpha=12)}$, where $\phi_{cr(\alpha=12)}$ is the ϕ_{cr} at $\alpha = 12$, with both values obtained at the same σ_3 . It can easily be noticed that the dispersion of ϕ_{cr} attains 10% at $\alpha < 12$, and gradually vanishes to $< 3\%$ beyond this threshold value.

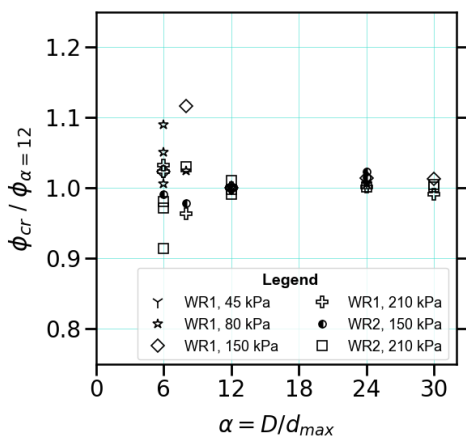


Figure 8. Normalized critical friction angle $\phi_{cr}/\phi_{cr(\alpha=12)}$ as a function of α .

4 CONCLUSIONS

A systematic study of numerical and physical experiments was presented to explore the effects of sample size on the critical shear strength of granular materials. Through triaxial test DEM simulations, it can be observed that the values of ϕ_{cr} stabilize when the sample scale $\alpha \geq 12$, regardless of the GSD. However, for better-graded samples, ϕ_{cr} reaches steady values as early as $\alpha = 8$. Laboratory triaxial tests also indicate that the critical shear strength is stable only if $\alpha \geq 12$, with significant dispersions for smaller α . These sample scales are bigger than what is indicated in widely used testing standards. Therefore, aspect ratio recommendations may not always ensure representative material characterization. This behavior may come from the formation of column-like structures mainly formed by the coarse fraction of the material (Cantor & Ovalle, 2023). Nonetheless, more extensive numerical and experimental testing is still needed to evaluate introducing new considerations in the testing standards.

It is important to note that while numerical work is not necessarily capable of replicating the complex soil behavior, it allows for an efficient study of specific mechanisms and effects, such as sample size assessments, under well-controlled conditions. Moreover, the parameters studied with DEM simulations in this work can be further analyzed to reveal the micro-mechanical sources of sample size effects, allowing for a better understanding of the mechanical behavior of granular soils.

5 ACKNOWLEDGEMENTS

This research work benefitted from the financial support of the Natural Sciences and Engineering Research Council of Canada (NSERC) [funding reference RGPIN-2019-06118], the Fonds de recherche du Quebec - Nature et technologies (FRQNT) [funding reference 2020-MN-281267], the industrial partners of the Research Institute on Mines and the Environment (RIME) UQAT-Polytechnique (www.irme.ca/en), Calcul Quebec and Digital Research Alliance of Canada.

6 REFERENCES

1. S. Amirpour Harehdasht, M. N. Hussien, M. Karray, V. Roubtsova, and M. Chekired, "Influence of particle size and gradation on shear strength-dilatation relation of granular materials," *Canadian Geotechnical Journal*, vol. 56, no. 2, pp. 208–227, Feb. 2019,
2. ASTM, *D7181 - Standard Test Method for Consolidated Drained Triaxial Compression Test for Soils*. ASTM International Standard, 2020.
3. E. Azéma, S. Linero, N. Estrada, and A. Lizcano, "Shear strength and microstructure of polydisperse packings: The effect of size span and shape of particle size distribution," *Physical Review E*, vol. 96, no. 2, Aug. 2017
4. E. Bard, M. Anabalón, and J. Campaña, "Waste rock behavior at high pressures.," in *Multiscale Geomechanics*. ISTE Wiley, 2012, pp. 83–112.
5. British Standard Institution, *BS 1377 British standard methods of test for soils for civil engineering purposes*. British Standard Institution, 1990.

6. D. Cantor, E. Azéma, and I. Preechawuttipong, "Microstructural analysis of sheared polydisperse polyhedral grains," *Physical review. E*, vol. 101, no. 6, Jun. 2020.
7. D. Cantor and C. Ovalle, "Sample size effects on the critical state shear strength of granular materials with varied gradation and the role of column-like local structures," *Géotechnique*, pp. 1–12, Dec. 2023,
8. S. Carrasco, D. Cantor, and C. Ovalle, "Effects of particle size-shape correlations on steady shear strength of granular materials: The case of particle elongation," *International journal for numerical and analytical methods in geomechanics*, vol. 46, no. 5, pp. 979–1000, Jan. 2022.
9. S. Carrasco, D. Cantor, C. Ovalle, and P. Quiroz-Rojo, "Shear strength of angular granular materials with size and shape polydispersity," *Open geomechanics*, vol. 4, pp. 1–14, Sep. 2023.
10. F. Dubois and M. Jean, "The non smooth contact dynamic method: recent LMGC90 software developments and application," *Springer eBooks*, pp. 375–378, Aug. 2006.
11. GDR MiDi, "On dense granular flows," *The European Physical Journal E*, vol. 14, no. 4, pp. 341–365, Aug. 2004.
12. G. Girumugisha, C. Ovalle, and S. Ouellet, "Sample Size Effect on Shear Strength of Mine Waste Rock Using the Scalping Method," Feb. 2024.
13. E. C. Hambly. A new true triaxial apparatus. *Géotechnique*, 19(2):307–309, 1969
14. Japanese Geotechnical Society, *JGS – 0520 Preparation of soil specimens for triaxial tests*. Japanese Geotechnical Society, 2020.
15. G. Li, C. Ovalle, C. Dano, and P. Y. Higher, "Influence of grain size distribution on critical state of granular materials," in *Constitutive Modeling of Geomaterials*, Heidelberg, Berlin: Springer Berlin Heidelberg, 2013, pp. 207–210.
16. S. Linero-Molina, C. Palma, and R. Apablaza, "Geotechnical Characterisation of Waste Material in Very High Dumps with Large Scale Triaxial Testing," *Proceedings of the 2007 International Symposium on Rock Slope Stability in Open Pit Mining and Civil Engineering*, 2007.
17. S. Linero-Molina, L. Bradfield, S. G. Fityus, J. V. Simmons, and A. Lizcano, "Design of a 720-mm Square Direct Shear Box and Investigation of the Impact of Boundary Conditions on Large-Scale Measured Strength," *Geotechnical Testing Journal*, vol. 43, no. 6, p. 20190344, Jun. 2020.
18. N. D. Marachi, C. K. Chan, and H. B. Seed, "Evaluation of Properties of Rockfill Materials," *Journal of the Soil Mechanics and Foundations Division*, vol. 98, no. 1, pp. 95–114, Jan. 1972.
19. H. Ouadfel and L. Rothenburg, "'Stress–force–fabric' relationship for assemblies of ellipsoids," *Mechanics of Materials*, vol. 33, no. 4, pp. 201–221, Apr. 2001.
20. C. Ovalle and C. Dano, "Effects of particle size–strength and size–shape correlations on parallel grading scaling," *Géotechnique Letters*, vol. 10, no. 2, pp. 191–197, Jun. 2020.
21. C. Ovalle, S. Linero, C. Dano, E. Bard, P. Hicher, and R. Osses, "Data Compilation from Large Drained Compression Triaxial Tests on Coarse Crushable Rockfill Materials," *Journal of geotechnical and geoenvironmental engineering*, vol. 146, no. 9, Sep. 2020.
22. C. Ovalle, G. Girumugisha, D. Cantor, and S. Ouellet, "Size effects assessment of mine waste-rock shear strength combining numerical, laboratory and in situ approaches," Jan. 2023.
23. F. Radjaï and F. Dubois, *Discrete-element modeling of granular materials*. London: Iste, 2011.
24. L. Valenzuela, E. Bard, J. Campaña, and M. Anabalón, "High Waste Rock Dumps — Challenges and Developments," in *Rock Dumps 2008: Proceedings of the First International Seminar on the Management of Rock Dumps, Stockpiles and Heap Leach Pads*, Perth: Australian Centre for Geomechanics, Jan. 2008, pp. 65–788.
25. J. Yang and X. D. Luo, "The critical state friction angle of granular materials: does it depend on grading?," *Acta Geotechnica*, vol. 13, no. 3, pp. 535–547, Aug. 2017.
26. J. Zeller and R. Wulliman, "The shear strength of the shell materials for the go-schenenalp dam, Switzerland," in *4th International Conference on Soil Mechanics and Foundation Engineering*, 1957, pp. 399–415.
27. J. Zheng and R. D. Hryciw, "Traditional soil particle sphericity, roundness and surface roughness by computational geometry," *Géotechnique*, vol. 65, no. 6, pp. 494–506, Jun. 2015.